The Journal of Chemical Physics

RESEARCH ARTICLE | JUNE 08 2020

Kapitza resistance at water–graphene interfaces

Sobin Alosious ; Sridhar Kumar Kannam ; Sarith P. Sathian ; B. D. Todd

Check for updates

J. Chem. Phys. 152, 224703 (2020)
https://doi.org/10.1063/5.0009001

View Online
Export Citation

Articles You May Be Interested In

Prediction of Kapitza resistance at fluid-solid interfaces

J. Chem. Phys. (November 2019)

Reverse nonequilibrium molecular dynamics simulation of thermal conductivity in nanoconfined polyamide-6,6

J. Chem. Phys. (August 2011)

Effects of interfacial molecular mobility on thermal boundary conductance at solid–liquid interface

J. Chem. Phys. (March 2023)

11 July 2026 17:14:52

AIP Publishing



The Journal of Chemical Physics ARTICLE scitation.org/journal/jcp

Kapitza resistance at water–graphene interfaces

Cite as: J. Chem. Phys. 152, 224703 (2020); doi: 10.1063/5.0009001
Submitted: 26 March 2020 • Accepted: 17 May 2020 •
Published Online: 8 June 2020

View Online Export Citation CrossMark

Sobin Alosious,[1,2] Sridhar Kumar Kannam,[2] Sarith P. Sathian,[1] and B. D. Todd[2,a)]

AFFILIATIONS

[1] Department of Applied Mechanics, Indian Institute of Technology Madras, Chennai 600036, India
[2] Department of Mathematics, Faculty of Science, Engineering and Technology, Swinburne University of Technology, Melbourne, Victoria 3122, Australia

[a)] Author to whom correspondence should be addressed: btodd@swin.edu.au

ABSTRACT

Heat transfer across fluid–solid interfaces in nanoconfinement has received significant attention due to its relevance in nanoscale systems. In this study, we investigate the Kapitza resistance at the water–graphene interface with the help of classical molecular dynamics simulation techniques in conjunction with our recently proposed equilibrium molecular dynamics (EMD) method [S. Alosious *et al.*, J. Chem. Phys. **151**, 194502 (2019)]. The size effect of the Kapitza resistance on different factors such as the number of graphene layers, the cross-sectional area, and the width of the water block was studied. The Kapitza resistance decreases slightly with an increase in the number of layers, while the influence of the cross-sectional area and the width of the water block is negligible. The variation in the Kapitza resistance as a function of the number of graphene layers is attributed to the large phonon mean free path along the graphene cross-plane. An optimum water–graphene system, which is independent of size effects, was selected, and the same was used to determine the Kapitza resistance using the predicted EMD method. The values obtained from both the EMD and the non-equilibrium molecular dynamics (NEMD) methods were compared for different potentials and water models, and the results are shown to be in good agreement. Our method allows us to compute the Kapitza resistance using EMD simulations, which obviates the need to create a large temperature gradient required for the NEMD method.

Published under license by AIP Publishing. https://doi.org/10.1063/5.0009001

11 July 2026 17:14:52

I. INTRODUCTION

In a previous paper, we developed an equilibrium molecular dynamics (EMD) method to compute the Kapitza resistance/length at fluid–solid interfaces and applied it to a sample Lennard-Jones (L-J) system.[1] The method was validated for different types of interfaces, density, channel width, and temperature and then compared with other approaches to compute the Kapitza resistance. The purpose of the present paper is to apply the theory to a more realistic system. A water–graphene system in which water is confined between a few graphene layers is used in this study.

Graphene has attracted significant attention as a novel two-dimensional substance in the last decade due to various captivating physical properties. Some of the remarkable properties of graphene are the superior thermal conductivity,[2,3] the high mechanical strength,[4] the high charge mobility,[5,6] and optical transparency.[7] In particular, the superior thermal conductivity of graphene[3] has triggered increasing efforts in the next-generation of electronic devices to develop graphene-based nanomaterials[8–10] for solving thermal management problems. Graphene has the potential to increase the thermal conductivity of nanofluids or nanocomposites; however, the interfacial thermal resistance or the Kapitza resistance between the graphene and the surrounding materials is a critical issue. To this end, water–graphene interfaces may have significant applications in nanoscale thermal management systems.

The water structure near a water/solid interface seems to be substantially different from the structure of water in bulk, and it can be propagated from the surface into considerable distances toward the bulk liquid.[11] Alexeev *et al.*[12] studied the effect of liquid layering on the Kapitza resistance between water and a few layers of graphene. They found that the Kapitza resistance is strongly dependent on the water layering adjacent to the graphene wall. They find it is inversely proportional to the first water density peak, which is consistent with better acoustic phonon matching between graphene and water. Ma *et al.*[13] found that interfacial charge decoration on graphene sheets leads to a considerable reduction in the Kapitza resistance at the water–graphene interface. The reduction in the interfacial thermal resistance is achieved by the increase in interaction strength caused by the increased Coulombic force between water and charged graphene sheets. Gonzalez-Valle *et al.*[14]

Published under license by AIP Publishing

studied the thermal transport across graphite–water interfaces. They found that the wetting response of an atomically dense surface can be described by the minimum of the adsorption energy curve, and a linear relationship can be obtained between binding energy and the work of adhesion. Also, the interfacial fluid depletion gives a sound reason for the correlation between wetting behavior and thermal transport. They have demonstrated the effect of different modeling techniques that affect heat transfer across fluid–solid interfaces. Pham *et al.*[15] examined the effect of pressure on the Kapitza resistance at gold/water and silicon/water interfaces. The pressure dependence of interfacial thermal resistance is found to be different for gold/water (hydrophilic) and silicon/water (hydrophobic) interfaces. Near the gold surface, the depletion length and peak value of the first water density layer are constant and independent of bulk liquid pressure. However, at the silicon surface, these values are directly related to bulk water pressure. These results show that the pressure dependence of the Kapitza resistance strongly depends on the type of the interface. Cao *et al.*[16] demonstrated that tuning of the Kapitza resistance at the water–graphene interface is possible by interlayer functionalization. Oxygen atoms were used for functionalization, and a reduction of about 50% in the Kapitza resistance is found for an oxygen ratio of 0.5%. They also found that the Kapitza resistance decreases with the addition of the number of layers owing to more overlapping of vibrational density of states at the interface.

Kapitza resistance studies on graphene–water interfaces are mostly carried out using non-equilibrium molecular dynamics (NEMD) methods. The NEMD method consists of an initial equilibration of the system at a reference temperature and followed by the addition and removal of heat from two ends of the system to obtain a linear temperature gradient across the system. By providing a temperature gradient, a temperature discontinuity will be formed at the interface due to the Kapitza resistance, and the Kapitza resistance can be directly calculated using this temperature drop at the interface and the applied heat flux. However, there is a considerably large value of temperature gradient required for calculating the Kapitza resistance using the NEMD method. This large temperature gradient might affect other properties that depend on temperature, and there are chances of inducing a nonlinear response that differs from the response that is of experimental interest. In addition to that, to obtain a linear temperature profile and steady-state heat flux, significant additional simulation time is required compared to our EMD method. In contrast, our EMD method uses correlation functions of heat flux and temperature difference at the interface in equilibrium to calculate the Kapitza resistance, eliminating the need for external driving forces and maintaining the system in steady-state, thereby saving computational time. The present work describes an EMD method to calculate the Kapitza resistance at the water–graphene interface utilizing both the heat flux and the temperature difference fluctuations at the interface. This method is an extension of our previous work in which we introduced a new approach to calculate the Kapitza resistance at a fluid–solid interface applied to an L-J system.[1] This paper consists of the methodology used to calculate the Kapitza resistance using our proposed EMD method. Furthermore, it includes detailed modeling of a water–graphene system and selection of different factors that affect the Kapitza resistance, such as the number of graphene layers, the thickness of the water channel, and the cross-sectional area of the graphene sheet. From this information, a suitable system is selected and the Kapitza length is calculated for different types of graphene potentials and water models. In what follows, we present a brief summary of the theory, modeling, and methodology used to simulate the system, an analysis of the results achieved, and some final conclusions.

II. THEORY

In this section, we briefly summarize the concept and the final expressions of the quantities of interest behind our EMD method for calculating the Kapitza resistance at fluid–solid interfaces. For full details, the reader is directed to the original paper.[1]

The Kaptiza resistance R_k, at the water-graphene interface, can be defined as follows:

$$R_k = \frac{\Delta T}{J_q}, \tag{1}$$

where $\Delta T = T_f - T_w$ is the temperature difference between the slab of water immediately adjacent to the wall, T_f, and the wall graphene layer, T_w, and J_q is the heat flux vector component normal to the wall. The average thickness of the slab of water is about one molecular diameter.

We assume that the time-dependent Kapitza kernel can be written as an n-term Maxwellian memory function and is given by[17]

$$R_k(t) = \sum_{i=1}^{n} k_i e^{-\mu_i t}, \tag{2}$$

where k_i and μ_i are the coefficients in the Maxwellian memory function. The coefficients k_i and μ_i are related by

$$\tilde{C}_{TJ_q}(s) = \sum_{i=1}^{n} \frac{k_i}{s+\mu_i} \tilde{C}_{J_qJ_q}(s), \tag{3}$$

where $\tilde{C}_{J_qJ_q}$ and $\tilde{C}_{TJ_q}$ are the Laplace transforms of the heat flux autocorrelation and the heat flux-temperature difference cross-correlation functions, respectively. For the steady-state conditions ($s = 0$), the Kapitza resistance, $\tilde{R}_k(0)$, can be computed by using the fitting parameters k_i and μ_i and is found to be

$$R_k \equiv \tilde{R}_k(0) = \sum_{i=1}^{n} \frac{k_i}{\mu_i}. \tag{4}$$

The instantaneous heat flux at a plane $J_{qz}(z, t)$ located at z, with surface area A, can be computed by the method of planes technique developed by Todd *et al.*:[18,19]

$$J_{qz}(z,t) = J^K_{qz}(z,t) + J^\phi_{qz}(z,t), \tag{5}$$

where $J^K_{qz}(z,t)$ and $J^\phi_{qz}(z,t)$ are the kinetic and the potential contributions of heat flux, respectively.

III. METHODOLOGY

The initial configuration of the system with water confined between a few graphene layers is shown in Fig. 1. This particular model consists of a water block with a dimension of $L \times L \times W$ and ten layers of graphene with a dimension of $L \times L$ on both the sides. The simulation domain was modeled in such a way that the density

11 July 2026 17:14:52

Published under license by AIP Publishing

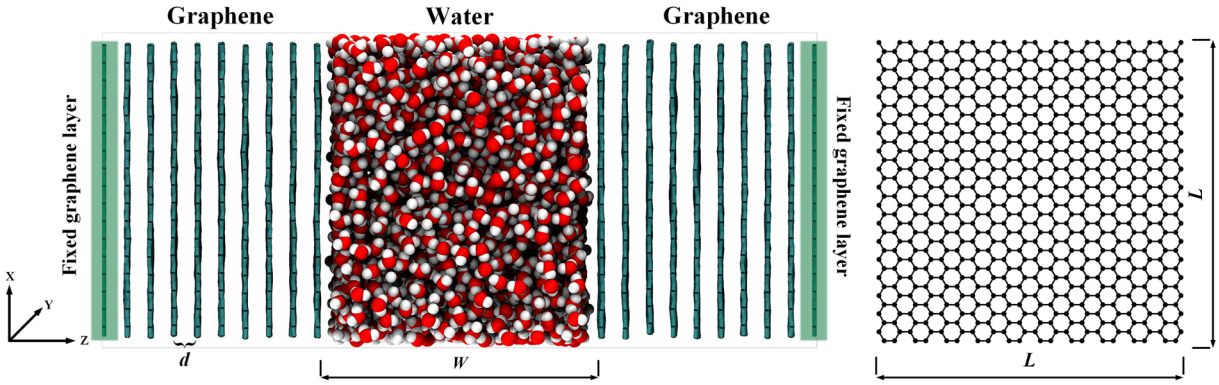


FIG. 1. Schematic diagram of the simulation domain.

at the mid-portion of the water block was maintained at the bulk density of water at 300 K by adjusting the number of water molecules inside the confinement. The size of the mid-portion was taken by avoiding the portion of water with considerable density fluctuation near both of the graphene layers. In a 4 nm water channel used in this study, the mid-portion consists of about 1.5 nm. The spacing between adjacent graphene layers was maintained at $d = 3.35$ Å.[20] Periodic boundary conditions were applied in the x-direction and y-direction and a fixed condition in the z-direction. The graphene layers at both ends were kept rigid to maintain a constant volume. To study the different factors affecting the calculation of the Kapitza resistance, different parameters in the model were varied, and a final model was selected based on that. The number of graphene layers on both sides was changed from 4 to 30. The cross-sectional area of a single graphene layer was varied by varying the size $L \times L$, from (2×2 nm^2) to (6×6 nm^2). In addition to that, the thickness of the water block, W, was varied from 2 nm to 8 nm.

The simple point charge (SPC/E)[21,22] water model was used to model the water molecules due to its reliability, accuracy, and relatively low computational cost. Also, a modified TIP3P[23,24] water model was used for comparison purposes due to its reproducibility of different thermodynamic properties. The water molecules were kept rigid using the SHAKE[25] algorithm, and the long-range electrostatic forces were computed using the particle–particle particle–mesh (PPPM)[26] solver with an accuracy of 1×10^{-5}. It is found that a higher accuracy of 1×10^{-6} consumes twice as much simulation time for less than 2% variation in the results. Due to the fixed boundary condition in the z-direction, an Ewald summation technique proposed by Yeh and Berkowitz[27] was followed with the ratio of the extended volume set as 3.0.

The intralayer carbon interactions were modeled by the adaptive intermolecular reactive empirical bond-order (AIREBO)[30] potential and an optimized Tersoff potential[31] for comparison. Also, the interlayer carbon interactions were modeled by the pairwise Lennard-Jones (L-J) potential, $\phi_{ij}(r) = 4\varepsilon\left[\left(\frac{\sigma}{r}\right)^{12} - \left(\frac{\sigma}{r}\right)^{6}\right]$, using the parameters from Girifalco *et al.*[29] The carbon–water interactions were modeled by L-J potentials with parameters taken from the work of Werder *et al.*,[28] with values of the L-J interaction parameters provided in Table I. The cutoff distance for the L-J potential and short-range Coulombic forces was set to 10 Å. All the simulations were performed using the Large-scale Atomic/Molecular Massively Parallel Simulator (LAMMPS)[32] package with a time step of 1.0 fs and visualized with the help of Visual Molecular Dynamics (VMD).[33]

For the NEMD simulations, the system was equilibrated under a canonical (NVT) ensemble for a time period of 2.0 ns after energy minimization. The system stability was verified by simulating under microcanonical ensemble conditions (NVE) for 2.0 ns. After that, a linear temperature gradient along the z-direction was created by adding and removing heat from both ends of the system, respectively. The heat addition and removal was achieved by maintaining two different temperatures (250 K and 350 K)[12] at two layers of graphene sheets each on both ends of the system (without considering fixed layers) by implementing a Langevin thermostat.[34] This process was continued for 6.0 ns until obtaining a linear temperature profile and a steady-state heat flux. Finally, the data were extracted from 5.0 ns production runs, from which the Kapitza resistance was calculated using Eq. (1).

For the EMD simulations, energy minimization, equilibration in the canonical ensemble, and system verification under the microcanonical ensemble were carried out similar to NEMD simulations. After that, the system was simulated at an equilibrium temperature of 300 K for 5.0 ns, by applying a Langevin thermostat only for graphene layers. During this simulation, the heat flux was calculated using Eq. (5), along with the temperature difference between the wall and the adjacent water slab. The Kapitza resistance was calculated using the proposed method described in Sec. II (see our original paper for details of this method[1]). Finally, the Kapitza length was

TABLE I. The L-J parameters used for modeling the water–graphene system.

Pair	σ (Å)	ε (kJ/mol)
O–O[22]	3.165	0.6503
C–O[28]	3.190	0.3920
C–C[29]	3.414	0.2313
H-all[22,28]	0.0	0.0

11 July 2026 17:14:52

Published under license by AIP Publishing

calculated using the equation $L_k = R_k\kappa$ for both the EMD and the NEMD methods, where κ can be the thermal conductivity of either water or graphene.[1] The Kapitza length toward the graphene side was calculated throughout this study by using the thermal conductivity of water at 300 K, which corresponds to the additional thickness of graphene required to achieve the same heat transfer in place of the thermal resistance at the interface (it is also possible to calculate the Kapitza length toward the water direction by using the thermal conductivity of graphene). The value of thermal conductivity of the SPC/E water model at 300 K, obtained using NEMD simulation, is $\kappa = 0.82 \pm 0.03$ W/K m, which is in agreement with previous results.[35–37]

IV. RESULTS AND DISCUSSION

Figure 2 is a typical temperature profile obtained from the NEMD simulations. The temperature jump ΔT at the interface due to the Kapitza resistance is clearly visible from the figure. The large temperature difference at the interface leading to a higher Kapitza length is an indication of poor heat transfer at water–graphene interfaces. For the NEMD method, R_k was directly calculated using Eq. (1).

To study the interfacial heat transfer using MD, a model that is free from size effects and uncertainties is essential. To prepare a suitable model, different factors affecting the Kapitza resistance were analyzed. Figure 3 shows the Kapitza length and the Kapitza resistance as a function of the cross-sectional area of the graphene layer. The value of the Kapitza length is found to be nearly constant for the selected cross-sectional areas. The inset in Fig. 3 shows the density profile near the interface for different cross-sectional areas. The density at the mid-portion was maintained at the bulk density of water for all the cases. The density profiles nearly coincide in all the cases, suggesting that there is no noticeable structural change in the alignment of water molecules near the interface irrespective of the cross-sectional area. A cross-sectional area of 4×4 nm^2 was chosen for all the cases in this study to balance between computational cost and uncertainty in the results.

To study the influence of the number of graphene layers on the Kapitza length/resistance, we have calculated the Kapitza length/resistance with a different number of graphene sheets on both sides. Figure 4(a) shows the dependency of the Kapitza length and the Kapitza resistance for a different number of graphene layers. Two different approaches were considered for this analysis. The first one was allowing the center of mass of the graphene layers to move along the z-direction freely (unconstrained), and the second approach was constraining the wall graphene layers to their initial center of mass positions (constrained). Note that, in all cases, individual carbon atoms are free to vibrate in their lattice structures.

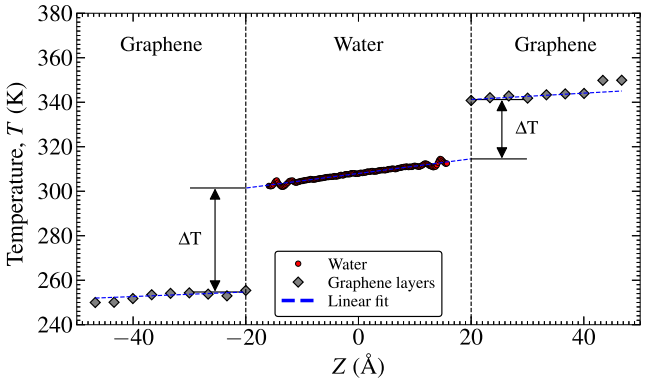


FIG. 2. Temperature profile obtained from NEMD simulations.

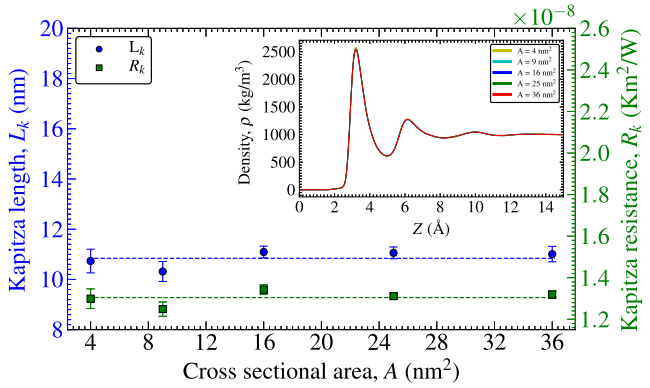


FIG. 3. The Kapitza length/resistance as a function of the cross-sectional area of the graphene layer. The inset shows the water density profile for different cross-sectional areas.

For the constrained approach, both the wall graphene layers were maintained at their initial positions by fixing the center of mass of the layers to their initial positions, which ensures a constant channel width. For the unconstrained case, it is found that the Kapitza length reduces with increasing the number of layers, and the slope decreases as the number of layers increases. A similar trend was reported by Alexeev *et al.*,[12] where the Kapitza resistance at the water–graphene interface monotonically decreases to an asymptotic value. However, when the wall graphene layers were constrained to their original position, it is found that the Kapitza length only slightly reduces with the addition of more graphene layers. Figures 4(b) and 4(c) show the density profile near the interface for constrained and unconstrained cases, respectively. For the unconstrained walls, the water block compresses as the number of graphene layers increases, leading to a reduction in water channel width. This compression of the water causes an increase in the first density peak of water, as seen in Fig. 4(c), which is the reason for the drastic reduction in the Kapitza length with the addition of graphene layers. The same effect is visible even if the system is equilibrated in the NPT ensemble initially by applying periodic boundary conditions in all directions. The increase in the first water density peak can also be achieved by increasing the system pressure, which again leads to a reduction in the Kapitza length.[12] On the other hand, from Fig. 4(b), it is clear that when the graphene walls are constrained to their initial center of mass positions, the density profiles nearly coincide irrespective of the number of graphene layers. This suggests that the number of graphene layers does not have much influence on the Kapitza length, and this contradicts the previously reported results.[12] Thus, the correct procedure is to constrain the graphene

11 July 2026 17:14:52

Published under license by AIP Publishing

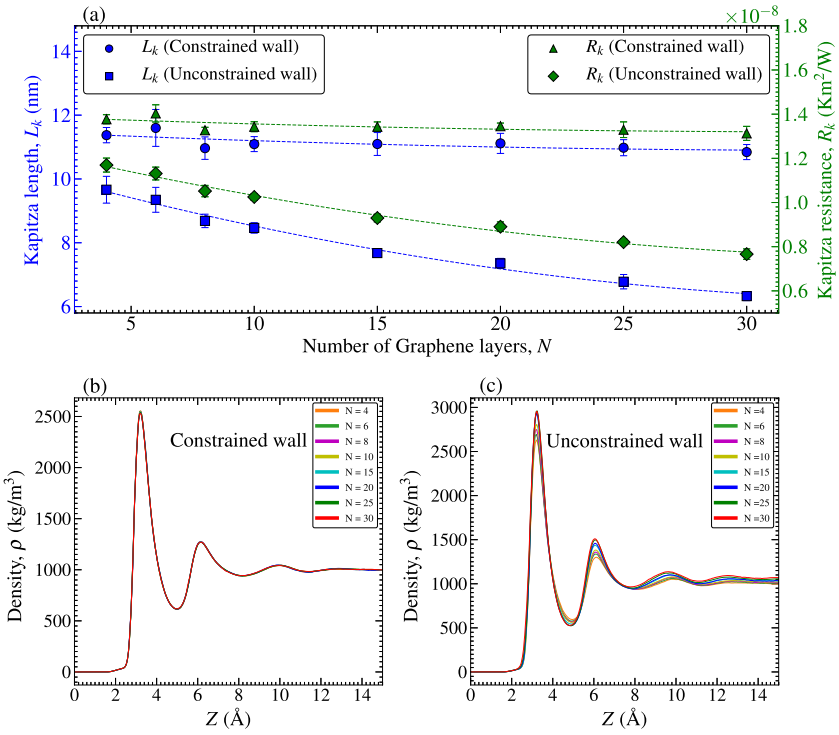


FIG. 4. The Kapitza length/resistance and corresponding water density profiles for a different number of graphene layers. (a) The Kapitza length/resistance as a function of the number of graphene layers for constrained and unconstrained walls. (b) The water density profile for a different number of graphene layers with walls constrained. (c) The water density profile for a different number of graphene layers with walls unconstrained.

walls to their initial center of mass positions so that the water does not compress, and the density of the water remains the same even if more graphene layers are added.

However, even after obtaining a similar density profile, there is still a slight reduction in the Kapitza length, which results from the size effects in the value of the Kapitza resistance and also due to the increase in the number of allowed phonon modes in graphene with an increase in the thickness. Liang *et al.*[38] reported the size effect of the Kapitza resistance in solid–solid interfaces. They found that the Kapitza resistance between a substrate and thin-film depends on the thickness of the film and the film surface roughness when the phonon mean free path is larger than the film thickness. From the acoustic mismatch model theory, the transmission coefficient at the interface is reduced when the thickness of the film is less than the phonon mean free path due to the specular reflection at the surface. Wei *et al.*[39] found that the phonon mean free path of the multilayer graphene along the cross-plane direction is higher than the thickness of graphene even after using 48 layers of graphene in their study. Thus, the slight reduction of the Kapitza length with the addition of the number of graphene layers can be attributed to the large phonon mean free path along the graphene cross-plane direction. Since the effect of the number of graphene layers has less influence, the selection of large numbers of graphene layers is not necessary compared to the high computational cost. We have, thus, selected N = 10 on both sides for all the cases in this study.

From Fig. 5, we can see that, unlike the wall thickness, the effect of water channel width when it is larger than 2 nm on the Kapitza resistance is found to be negligible with the constrained wall approach. The density profile in the inset shows that the structure of the water remains nearly the same for all the channel widths. Even though the Kapitza resistance is a function of water structure, the abovementioned results show that the Kapitza resistance is only affected by the structure of water close to the interface, and the bulk portion has a negligible effect. In addition to this, the mean free path of water is very small (≈2.5 Å)[40] compared to the lowest channel width; therefore, the size effect can be neglected.

Based on the abovementioned observations, a suitable water–graphene model, which is independent of size effects and relatively

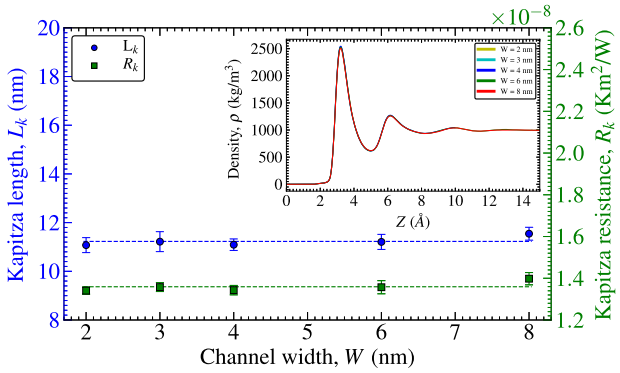


FIG. 5. The Kapitza length/resistance as a function of the different water channel widths. The inset shows the water density profile for different water channel widths.

11 July 2026 17:14:52

Published under license by AIP Publishing

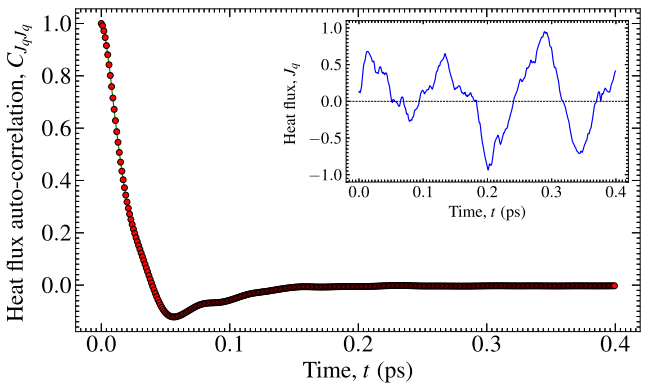


FIG. 6. The normalized heat flux autocorrelation function. The inset shows the fluctuation of the normalized heat flux at the interface as a function of time.

low uncertainties, was selected, and the Kapitza resistance was calculated using the predicted EMD method. The model consists of 10 layers of graphene with a cross-sectional area of 4×4 nm^2 placed on both sides of a 4 nm length water block. The reference temperature is taken as 300 K. Figure 6 shows the normalized auto-correlation function, $C_{J_qJ_q}$, of the heat flux across the water–graphene interface. The inset shows the fluctuation of the normalized heat flux at the interface as a function of time for a time interval of 0.4 ps. The autocorrelation function was calculated using this heat flux data, averaged over 5.0 ns. The correlation function decays to zero at a time interval of about 0.2 ps.

Similarly, the normalized heat flux-temperature difference cross-correlation function, C_{J_qT}, is plotted in Fig. 7. The inset shows the fluctuation of the temperature difference between graphene and water at the interface as a function of time for a time interval of 0.4 ps. The cross-correlation was calculated using this temperature difference data, and the heat flux data averaged over 5.0 ns. The heat flux and temperature difference are anticorrelated initially because the heat flux flows in the direction opposite to the temperature difference. The cross-correlation functions decay to zero after a time span of around 0.2 ps. The Laplace transform of both the correlation functions was calculated using a simple trapezoidal integration method, and the corresponding data were fitted using Eq. (3). The fitting parameters μ_i and k_i in Eq. (3) are obtained with a Maxwellian one term ($n = 1$) memory function, which has been shown to be sufficient in previous studies.[1,41] Finally, the Kapitza resistance was calculated using Eq. (4).

The instantaneous temperature difference at the interface was calculated by measuring the difference in temperature of the wall graphene layer and a slab of water adjacent to the wall graphene layer. The selection of water slab thickness Δ, is a crucial factor in the calculation of the Kapitza resistance. Kannam *et al.*[42] used a one molecular diameter slab thickness for calculating slip length at the water–graphene interface. Figure 8 shows the Kapitza length and the Kapitza resistance as a function of the water slab thickness, and the inset shows the selected slab thickness Δ and the water density profile. For the case of Kapitza resistance, we found that the cross-correlation function converges smoothly when Δ is near to the first peak of the water density, which is about one molecular diameter. From Fig. 8, we can see that the value of the Kapitza length is inconsistent for smaller values of the Δ due to insufficient water molecules to compute the properties of the slab and then slowly decreases as the slab thickness increases. However, for higher slab thickness, the properties computed will be bulk properties, whereas the Kapitza resistance is an interfacial property. Thus, by considering these factors, we have chosen an optimum water slab thickness as Δ = 3.165 Å, which is the distance from the graphene wall to the first density peak of water. At Δ = 3.165 Å, the cross-correlation function converges smoothly, and the Kapitza length reaches a consistent value.

Finally, our EMD method is compared with the NEMD method for different graphene potentials and water models. Figure 9 shows the comparison of the Kapitza length calculated using our EMD method and the NEMD method for different cases. The AIREBO potential consumes about three times more computational time compared to the Tersoff potential, and a 5.06% difference in results was observed. Regarding the water models, the SPC/E water model is widely used due to its reproducibility of different properties of

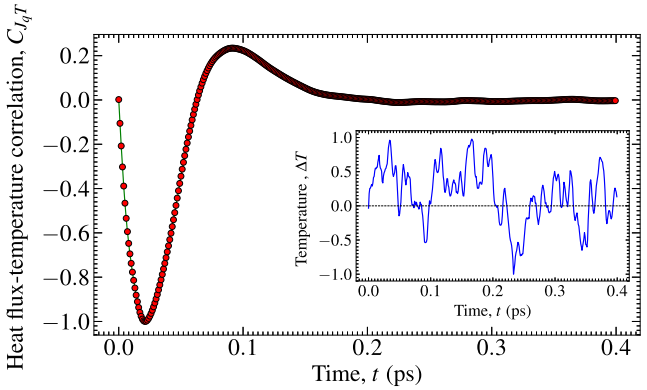


FIG. 7. The normalized temperature difference-heat flux cross-correlation function. The inset shows the fluctuation of the temperature difference between graphene and water at the interface as a function of time.

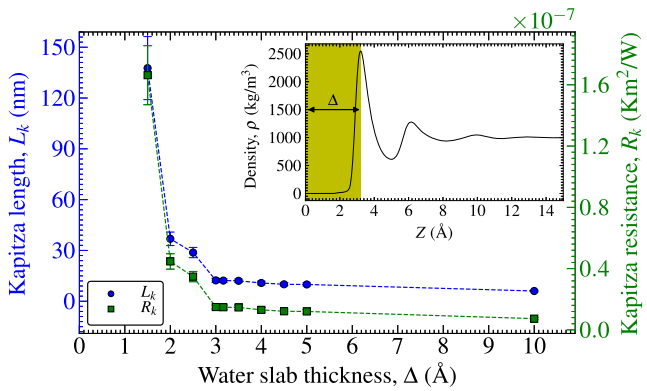


FIG. 8. The Kapitza length/resistance as a function of water slab thickness. The inset shows the selected slab thickness, Δ, and the density profile of water.

11 July 2026 17:14:52

Published under license by AIP Publishing

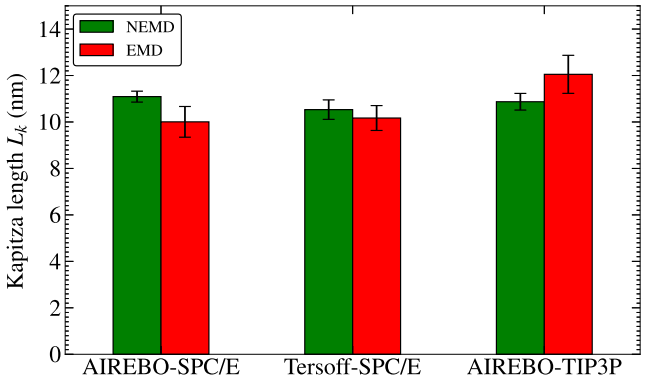


FIG. 9. Comparison of the predicted value of the Kapitza length with the NEMD simulations for different graphene potentials and water models.

TABLE II. The Kapitza resistance values for the water–graphene interface for different graphene potentials and water models at 300 K.

Model	NEMD R_k ($\times 10^{-8}$ K m^2/W)	EMD R_k ($\times 10^{-8}$ K m^2/W)
AIREBO-SPC/E	1.343 ± 0.028	1.212 ± 0.080
Tersoff-SPC/E	1.275 ± 0.050	1.231 ± 0.064
AIREBO-TIP3P	1.316 ± 0.043	1.459 ± 0.099

water. A 2.01% difference in results was observed when the TIP3P water model was used. In all three cases, the results obtained from our EMD method are in excellent agreement with the results of the NEMD method. The Kapitza resistance values of all the cases are provided in Table II. A wide range of values of the Kapitza resistance at the water–graphene interface ranging from 0.8×10^{-8} K m^2/W to 6.2×10^{-8} K m^2/W are reported in different articles.[12–14,43,44] This wide range of values is due to the different factors affecting the Kapitza resistance, such as the selection of the system, type of the water model, type of potential, wettability at the interface, number of layers, temperature, and pressure. Also, one of the significant factors is the density of water inside the channel, especially, the first density peak. The different MD techniques used to fill water inside a graphene nanochannel result in variation in density inside the channel, which is a major deciding factor for the value of the Kapitza resistance.

V. CONCLUSION

In summary, we have studied the Kapitza resistance at a water–graphene interface using molecular dynamics simulations, in which the water is confined between a few layers of graphene sheets. NEMD and EMD simulation techniques were used to compute the Kapitza resistance. The size effect of the Kapitza resistance on various factors such as the number of graphene layers, cross-sectional area, and the water channel width was investigated. It is found that the Kapitza resistance decreases slightly with an addition of graphene layers. The dependency of the Kapitza resistance on the number of graphene layers is due to the large phonon mean free path along the graphene cross-plane. The results show that the water channel width and the graphene cross-sectional area have a negligible influence on the Kapitza resistance. In addition to that, the water density structure close to the interface nearly coincides with different channel widths and cross-sectional areas. From these observations, we can infer that the structure of water near the interface, especially the first density peak, plays a significant role in the heat transfer across the interface.[12]

The selection of a reliable model is essential for the prediction of the Kapitza resistance using MD techniques to obtain reliable results. From the abovementioned observation, a suitable model was selected, which is free from size effects with reasonable uncertainties, and this model was used for further analyses. In a previous paper, we introduced a new EMD method to calculate the Kapitza resistance using the heat flux autocorrelation function and the heat flux-temperature difference cross-correlation function in a system with L-J particles. We extended this method to a realistic system, which consists of a block of water confined between a few layers of graphene sheets. The method was again validated by comparing the EMD results with NEMD results for different graphene potentials and water models, and both the results are in excellent agreement. For the NEMD method, a large temperature gradient of about 5–17 K/nm (corresponds to the different number of graphene layers) is required to obtain a steady-state temperature profile and to collect sufficient statistics. This temperature gradient is achieved by applying a heat flux across the interface by addition and removal of heat from both ends of the system. The Kapitza resistance is calculated using this applied heat flux and the resulting temperature-difference at the interface using Eq. (1). Here, we are assuming that the heat flux and temperature difference are linearly proportional to each other for a particular interface. However, there is a possibility of deviation from this linear dependency for relatively large temperature gradients (hence, large heat fluxes). For interfaces with very low Kapitza resistance, we are forced to apply a very high value of heat flux to obtain a noticeable temperature-difference at the interface. Thus, for such systems with a high value of applied heat flux, the temperature-difference at the interface may deviate from the assumed linear form, and this will be reflected in the calculated value of the Kapitza resistance. In addition to this, a higher temperature-difference at the interface will also affect the value of the calculated Kapitza resistance since the Kapitza resistance is a temperature-dependent property.[1] This limitation does not influence our EMD method since it evaluates only the linear response of the system. In addition to that, to obtain a steady-state temperature profile, an additional 6.0 ns time is required for the NEMD method. Also, the NEMD method we have used in this paper cannot be feasible for confined fluids under flow conditions because creating such a steady-state linear temperature profile is not possible for such systems. Similarly, for the case of fluids (with or without flow) confined in cylindrical nanopores such as carbon nanotubes (CNTs), creating a linear temperature gradient across the interface is not possible. This is because if we follow the current NEMD method of applying two different temperatures to obtain a linear temperature gradient, we need to longitudinally divide the cylindrical nanopores into two parts and apply two different temperatures to these two parts. Thus, the adjacent atoms, which are bonded to

11 July 2026 17:14:52

Published under license by AIP Publishing

each other along the longitudinal division, will be forced to have two different temperatures, which is an unrealistic situation. This limitation restricts the use of the current NEMD method in cylindrical nanopores. Furthermore, under flow conditions (e.g., Poiseuille flow), the temperature profile may be very weakly quartic and almost flat, which may lead to an unrealistic Kapitza length of $L_k \to \infty$ if we extrapolate the interfacial temperature back into the wall. For these reasons, we propose that the EMD method is better for calculating the Kapitza resistance in the abovementioned scenarios. In future work, we will extend our EMD method for computing the Kapitza resistance in fluids confined in graphene channels and carbon nanotubes under flow conditions, where NEMD methods are likely to be difficult to use for systems with high slip.

ACKNOWLEDGMENTS

The authors acknowledge the Swinburne University Supercomputer Centre for providing computational resources for this work.

DATA AVAILABILITY

The data that support the findings of this study are available from the corresponding author upon reasonable request.

REFERENCES

[1]S. Alosious, S. K. Kannam, S. P. Sathian, and B. D. Todd, "Prediction of Kapitza resistance at fluid-solid interfaces," J. Chem. Phys. **151**, 194502 (2019).
[2]A. A. Balandin, S. Ghosh, W. Bao, I. Calizo, D. Teweldebrhan, F. Miao, and C. N. Lau, "Superior thermal conductivity of single-layer graphene," Nano Lett. **8**, 902–907 (2008).
[3]A. A. Balandin, "Thermal properties of graphene and nanostructured carbon materials," Nat. Mater. **10**, 569 (2011).
[4]C. Lee, X. Wei, J. W. Kysar, and J. Hone, "Measurement of the elastic properties and intrinsic strength of monolayer graphene," Science **321**, 385–388 (2008).
[5]S. Morozov, K. Novoselov, A. Geim, D. Jiang, Y. Zhang, S. Dubonos, I. Grigorieva, A. Firsov, and J. Mussell, "Electric field effect in atomically thin carbon films," Science **306**, 666 (2004).
[6]Y. Zhang, Y.-W. Tan, H. L. Stormer, and P. Kim, "Experimental observation of the quantum Hall effect and Berry's phase in graphene," Nature **438**, 201 (2005).
[7]R. R. Nair, P. Blake, A. N. Grigorenko, K. S. Novoselov, T. J. Booth, T. Stauber, N. M. Peres, and A. K. Geim, "Fine structure constant defines visual transparency of graphene," Science **320**, 1308 (2008).
[8]J. Chen, J. H. Walther, and P. Koumoutsakos, "Covalently bonded graphene–carbon nanotube hybrid for high-performance thermal interfaces," Adv. Funct. Mater. **25**, 7539–7545 (2015).
[9]J. Chen, J. H. Walther, and P. Koumoutsakos, "Strain engineering of Kapitza resistance in few-layer graphene," Nano Lett. **14**, 819–825 (2014).
[10]J. Chen, J. H. Walther, and P. Koumoutsakos, "Ultrafast cooling by covalently bonded graphene-carbon nanotube hybrid immersed in water," Nanotechnology **27**, 465705 (2016).
[11]W. Drost-Hansen, "Structure of water near solid interfaces," Ind. Eng. Chem. **61**, 10–47 (1969).
[12]D. Alexeev, J. Chen, J. H. Walther, K. P. Giapis, P. Angelikopoulos, and P. Koumoutsakos, "Kapitza resistance between few-layer graphene and water: Liquid layering effects," Nano Lett. **15**, 5744–5749 (2015).
[13]Y. Ma, Z. Zhang, J. Chen, K. Sääskilahti, S. Volz, and J. Chen, "Ordered water layers by interfacial charge decoration leading to an ultra-low Kapitza resistance between graphene and water," Carbon **135**, 263–269 (2018).
[14]C. U. Gonzalez-Valle, L. E. Paniagua-Guerra, and B. Ramos-Alvarado, "Implications of the interface modeling approach on the heat transfer across graphite–water interfaces," J. Phys. Chem. C **123**, 22311–22323 (2019).
[15]A. Pham, M. Barisik, and B. Kim, "Pressure dependence of Kapitza resistance at gold/water and silicon/water interfaces," J. Chem. Phys. **139**, 244702 (2013).
[16]B.-Y. Cao, J.-H. Zou, G.-J. Hu, and G.-X. Cao, "Enhanced thermal transport across multilayer graphene and water by interlayer functionalization," Appl. Phys. Lett. **112**, 041603 (2018).
[17]D. J. Evans and G. Morriss, *Statistical Mechanics of Nonequilibrium Liquids* (Cambridge University Press, 2008).
[18]B. D. Todd and P. J. Daivis, *Nonequilibrium Molecular Dynamics: Theory, Algorithms and Applications* (Cambridge University Press, 2017).
[19]B. D. Todd, P. J. Daivis, and D. J. Evans, "Heat flux vector in highly inhomogeneous nonequilibrium fluids," Phys. Rev. E **51**, 4362 (1995).
[20]G. A. Slack, "Anisotropic thermal conductivity of pyrolytic graphite," Phys. Rev. **127**, 694 (1962).
[21]H. J. Berendsen, J. Grigera, and T. Straatsma, "The missing term in effective pair potentials," J. Phys. Chem. **91**, 6269–6271 (1987).
[22]Y. Wu, H. L. Tepper, and G. A. Voth, "Flexible simple point-charge water model with improved liquid-state properties," J. Chem. Phys. **124**, 024503 (2006).
[23]W. L. Jorgensen, J. Chandrasekhar, J. D. Madura, R. W. Impey, and M. L. Klein, "Comparison of simple potential functions for simulating liquid water," J. Chem. Phys. **79**, 926–935 (1983).
[24]D. J. Price and C. L. Brooks III, "A modified TIP3P water potential for simulation with Ewald summation," J. Chem. Phys. **121**, 10096–10103 (2004).
[25]J.-P. Ryckaert, G. Ciccotti, and H. J. Berendsen, "Numerical integration of the Cartesian equations of motion of a system with constraints: Molecular dynamics of *n*-alkanes," J. Comput. Phys. **23**, 327–341 (1977).
[26]R. W. Hockney and J. W. Eastwood, *Computer Simulation Using Particles* (CRC Press, 1988).
[27]I.-C. Yeh and M. L. Berkowitz, "Ewald summation for systems with slab geometry," J. Chem. Phys. **111**, 3155–3162 (1999).
[28]T. Werder, J. H. Walther, R. Jaffe, T. Halicioglu, and P. Koumoutsakos, "On the water–carbon interaction for use in molecular dynamics simulations of graphite and carbon nanotubes," J. Phys. Chem. B **107**, 1345–1352 (2003).
[29]L. Girifalco, M. Hodak, and R. S. Lee, "Carbon nanotubes, buckyballs, ropes, and a universal graphitic potential," Phys. Rev. B **62**, 13104 (2000).
[30]S. J. Stuart, A. B. Tutein, and J. A. Harrison, "A reactive potential for hydrocarbons with intermolecular interactions," J. Chem. Phys. **112**, 6472–6486 (2000).
[31]L. Lindsay and D. Broido, "Optimized Tersoff and Brenner empirical potential parameters for lattice dynamics and phonon thermal transport in carbon nanotubes and graphene," Phys. Rev. B **81**, 205441 (2010).
[32]S. Plimpton, "Fast parallel algorithms for short-range molecular dynamics," J. Comput. Phys. **117**, 1–19 (1995).
[33]W. Humphrey, A. Dalke, and K. Schulten, "VMD: Visual molecular dynamics," J. Mol. Graphics **14**, 33–38 (1996).
[34]G. S. Grest and K. Kremer, "Molecular dynamics simulation for polymers in the presence of a heat bath," Phys. Rev. A **33**, 3628 (1986).
[35]T. W. Sirk, S. Moore, and E. F. Brown, "Characteristics of thermal conductivity in classical water models," J. Chem. Phys. **138**, 064505 (2013).
[36]M. Zhang, E. Lussetti, L. E. de Souza, and F. Müller-Plathe, "Thermal conductivities of molecular liquids by reverse nonequilibrium molecular dynamics," J. Phys. Chem. B **109**, 15060–15067 (2005).
[37]H. Jiang, E. M. Myshakin, K. D. Jordan, and R. P. Warzinski, "Molecular dynamics simulations of the thermal conductivity of methane hydrate," J. Phys. Chem. B **112**, 10207–10216 (2008).

11 July 2026 17:14:52

Published under license by AIP Publishing

[38]Z. Liang, K. Sasikumar, and P. Keblinski, "Thermal transport across a substrate–thin-film interface: Effects of film thickness and surface roughness," Phys. Rev. Lett. **113**, 065901 (2014).
[39]Z. Wei, Z. Ni, K. Bi, M. Chen, and Y. Chen, "Interfacial thermal resistance in multilayer graphene structures," Phys. Lett. A **375**, 1195–1199 (2011).
[40]S. Chapman, T. G. Cowling, and D. Burnett, *The Mathematical Theory of Non-Uniform Gases: An Account of the Kinetic Theory of Viscosity, Thermal Conduction and Diffusion in Gases* (Cambridge University Press, 1990).
[41]J. S. Hansen, B. Todd, and P. J. Daivis, "Prediction of fluid velocity slip at solid surfaces," Phys. Rev. E **84**, 016313 (2011).
[42]S. Kumar Kannam, B. Todd, J. S. Hansen, and P. J. Daivis, "Slip length of water on graphene: Limitations of non-equilibrium molecular dynamics simulations," J. Chem. Phys. **136**, 024705 (2012).
[43]A. T. Pham, M. Barisik, and B. Kim, "Interfacial thermal resistance between the graphene-coated copper and liquid water," Int. J. Heat Mass Transfer **97**, 422–431 (2016).
[44]F. Jabbari, A. Rajabpour, S. Saedodin, and S. Wongwises, "Effect of water/carbon interaction strength on interfacial thermal resistance and the surrounding molecular nanolayer of CNT and graphene flake," J. Mol. Liq. **282**, 197–204 (2019).

11 July 2026 17:14:52

Published under license by AIP Publishing